

Highly-Nonlinear Silicon Photonics Slot Waveguide

C. Koos¹, P. Vorreau¹, P. Dumon², R. Baets², B. Esembeson³, I. Biaggio³,
T. Michinobu⁴, F. Diederich⁴, W. Freude¹, and J. Leuthold¹

¹Institute of High-Frequency and Quantum Electronics, University of Karlsruhe, 76131 Karlsruhe, Germany

²Photonics Research Group, Ghent University, B-9000 Gent, Belgium

³Department of Physics, Lehigh University, Bethlehem, PA 18015, USA

⁴Laboratorium für Organische Chemie, ETH Zürich, Hönggerberg, HCI, CH-8093 Zürich, Switzerland

Email: C.Koos@ihq.uka.de; J.Leuthold@ihq.uka.de

Abstract: A silicon photonics slot waveguide with a record nonlinearity of $104\,000\text{ W}^{-1}\text{km}^{-1}$ at $1.5\text{ }\mu\text{m}$ is reported. We demonstrate demultiplexing of 130 Gbit/s signals to 10 Gbit/s using FWM in a 6 mm-long device.

©2008 Optical Society of America

OCIS codes: (130.4310) Nonlinear; (130.2790) Guided Waves; (160.4330) Nonlinear optical materials; (190.3270) Kerr effect; (190.4710) Optical nonlinearities in organic materials; (190.5970) Semiconductor nonlinear optics.

1. Introduction

Highly nonlinear fibers and nonlinear semiconductor waveguides are key for all-optical signal processing at speeds beyond the limits of electronics. Many promising nonlinear materials like semiconductor optical amplifiers, organic materials, doped glasses and recently also chalcogenide glasses have been studied. An advantage of Kerr effect based organic materials and glasses is the ultrafast response time on the scale of 10 fs; yet, the effect itself is weak requiring long interaction lengths. Typical nonlinear fibers have nonlinearity coefficients in the order of $10\text{--}20\text{ W}^{-1}\text{km}^{-1}$ calling for fiber lengths in the order of hundreds of meters with peak powers in the order of watt. Holey fibers concentrate the optical field strongly to the core leading to effective nonlinearities of $\gamma = 1\,860\text{ W}^{-1}\text{km}^{-1}$ [1] or even $\gamma = 68\,000\text{ W}^{-1}\text{km}^{-1}$ in an 18 mm piece of tapered chalcogenide subwavelength-diameter fiber [2].

Future silicon photonics calls for integratable Kerr-nonlinear devices. And indeed, a serpentine-shaped 22 cm long chalcogenide glass planar waveguide, folded on a 7 cm long chip, showed a nonlinearity coefficient of $1\,700\text{ W}^{-1}\text{km}^{-1}$ [3]. Yet, the ultimate small-scale integratable device should be based on the mature silicon platform and on standard lithographic CMOS processes. The device should allow operation over a large wavelength range and should not require dispersion management. While 10 Gbit/s FWM in silicon wires has been shown [4], there is the potential influence of two-photon absorption and free carrier generation at higher peak powers and bitrates, which would impede optical signal processing at high speed and requires measures to remove the free carriers [5].

In this paper, we report on an integrated organic-silicon-on-insulator (SOI) compound waveguide with a nonlinearity of $104\,000\text{ W}^{-1}\text{km}^{-1}$. This is, to the best of our knowledge, the highest nonlinear coefficient ever reported for nanophotonic SOI slot waveguides. In a proof of principle experiment, a device of 6 mm length has been successfully tested for its capability to demultiplex a 130 Gbit/s signal to 10 Gbit/s by FWM. This nonlinearity was achieved with a slotted waveguide fabricated by standard CMOS technology. The optical mode was strongly confined to a slot filled with a highly nonlinear organic compound showing only little two-photon absorption.

2. Highly Nonlinear SOI Slot Waveguides and Optimization for Maximum Nonlinearity

The structure of the highly nonlinear silicon on insulator slot waveguide is shown in Fig. 1(a). Its core consists of two silicon (Si) ribs on a silicon buffer (SiO_2). The slot waveguide is filled and covered with a Kerr-type nonlinear organic cladding (NL).

To maximize the nonlinearity we need to optimize the nonlinear parameter $\gamma = (n_2 k_0) / A_{\text{eff}}^{(3)}$, where the effective area of nonlinear interaction $A_{\text{eff}}^{(3)}$ depends on the waveguide geometry, the quantity k_0 denotes the free-space wave number, and n_2 is the intensity-related nonlinear index coefficient.

In a first step we optimized the waveguide geometry for maximum confinement of the optical mode in the slot. By varying the rib width w and height h and by limiting ourselves to technologically realizable slot widths of $w_{\text{slot}} \geq 60\text{ nm}$, the area $A_{\text{eff}}^{(3)}$ can become significantly smaller than $0.1\text{ }\mu\text{m}^2$, Fig.1(b). The field intensity has been further enhanced (Fig. 1(b) [6]) by choosing an organic slot material with the smallest refractive index available. This results in a four-fold field enhancement due to the discontinuity of the normal electric field component at the interface of silicon (refractive index 3.48) and the organic material with (refractive index 1.69). We then choose an organic material with a high nonlinear coefficient and a low two-photon absorption. For the structure outlined below, we then obtain a nonlinearity coefficient in the order of $\gamma=100\,000\text{ W}^{-1}\text{km}^{-1}$.

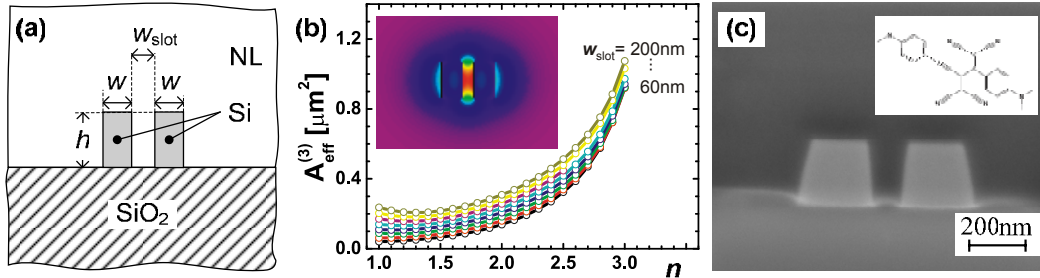


Fig. 1 (a) Cross section of an SOI slot waveguide; it consists of two silicon (Si) ribs on a silicon dioxide buffer layer (SiO_2) and is covered by a nonlinear material (NL). (b) Effective area for nonlinear interaction as a function of the linear refractive index n_{NL} of the nonlinear cover material. Strip width w and waveguide height h have been optimized for fixed slot widths w_{slot} . Inset: Field plot of the dominant electric field component (E_x) for a slot width $w_{\text{slot}} = 100$ nm and $n_{\text{NL}} = 1.5$. (c) Cross section of a fabricated slot waveguide functionalized with an organic film; Inset: Molecular structure of the nonlinear organic material.

3. Fabrication of SOI Waveguide Templates and Functionalization with Organic $\chi^{(3)}$ -Materials

The SOI templates have been fabricated on a 200 mm CMOS line using 193 nm DUV lithography on an ASML PAS5500/1100 stepper and Cl-based reactive ion etching [7]. The thickness of the SOI device layer (waveguide height) was $h = 220$ nm, and the buried oxide is 2 μm thick. The strip (slot) widths w (w_{slot}) range from 160 nm to 220 nm (150 nm to 250 nm). The waveguides were functionalized by vapour deposition of an amorphous organic film of 950 nm thickness. The film consists of DDMEBT (2-[4-(Dimethylamino)phenyl]-3-[[4-(dimethylamino)phenyl]ethynyl]buta-1,3-diene-1,1,4,4-tetracarbonitrile). The molecules are described in more detail as derivative 2 in [9], and the structure is depicted in the inset of Fig. 1(c). The refractive index of the organic film is $n = 1.69$, and the nonlinear index coefficient amounts to $n_2 = 1.69 \times 10^{-17} \text{ m}^2 / \text{W}$. Cross-sectional profiles of the waveguides have been produced by focussed ion beam (FIB) milling, see Fig. 1(c). It was found that the organic material was nicely deposited into the slot without forming any voids. The Si ribs exhibit a slightly trapezoidal shape.

4. Sample Characterization

For a slot waveguide of height $h = 220$ nm, width $w = 216$ nm and slot width $w_{\text{slot}} = 157$ nm, the fiber-chip coupling losses amount to $a_{\text{cp}} = 3.8$ dB per facet and the propagation loss is 2.3 dB/mm ($\alpha = 0.53/\text{mm}$) at 1550 nm. This results in an effective nonlinear interaction length of $L_{\text{eff}} = (1 - \exp(-\alpha L)) / \alpha = 1.89 \text{ mm}$ for the 5.99 mm long waveguide.

The nonlinear parameter γ was obtained by measuring the conversion efficiency $\eta = \exp(-\alpha L) (\gamma P_p L_{\text{eff}})^2$ of degenerate four-wave mixing (FWM) with continuous-wave pump and signal, where P_p denotes the on-chip pump power at the begin of the waveguide. Measuring two different samples with nominally identical geometry at two different signal wavelengths, we have obtained nonlinear parameters γ of $116\,000 \text{ W}^{-1} \text{ km}^{-1}$, $107\,000 \text{ W}^{-1} \text{ km}^{-1}$, $104\,000 \text{ W}^{-1} \text{ km}^{-1}$ and $91\,000 \text{ W}^{-1} \text{ km}^{-1}$, leading to an average value of $104\,000 \text{ W}^{-1} \text{ km}^{-1}$.

A dispersion parameter of $D = 1/c \times dn_{\text{eg}} / d\lambda = -9.21 \text{ fs}/(\text{mm nm})$ was derived from the Fabry-Perot resonances in the transmission spectrum. For wavelength conversion over 20 nm, the corresponding coherence length over which the signal and the converted wave accumulate a phase shift of π is hence $L_{\text{coh}} = 4.34$ mm, and it can be concluded that the conversion efficiency is limited rather by waveguide loss than by dispersion.

5. All-Optical Demultiplexing

To proof the viability of the concept we performed all-optical demultiplexing of a 120 Gbit/s to a 10 Gbit/s data stream. The experimental setup together with the eye diagrams are depicted in Fig. 2. For the data (pump) we used mode-locked fiber lasers operating at repetition rates of 40 GHz (10 GHz) and emitting pulses of approximately 3 ps FWHM. The signal and the pump were synchronized using a tuneable optical delay. The 120 Gbit/s data were generated by modulating the 40 GHz pulse train with a pseudo-random bit sequence (2^{31} -1 bit) and by subsequent optical time-division multiplexing. Both the pump and the signal are amplified and coupled into a SOI slot waveguide of height $h = 220$ nm, strip width $w = 212$ nm and slot width $w_{\text{slot}} = 205$ nm. The output signal was bandpass-filtered at the converted wavelength, amplified and the eye diagram was recorded with a digital communication analyzer. By varying the delay between the pump and the signal, different tributaries could be demultiplexed. Similar performances were found for the different tributaries. From the eye diagram, a Q-factor of $Q^2 = 11.1$ dB was measured for an on-chip pump power of 15.6 dBm (36 mW). Since the power of the converted

signal depends quadratically on the pump power, and since the 10 GHz pump exhibits noticeable amplitude fluctuations (see eye diagram (2) in Fig. 3), the Q-factor was mainly limited by the performance of the pump.

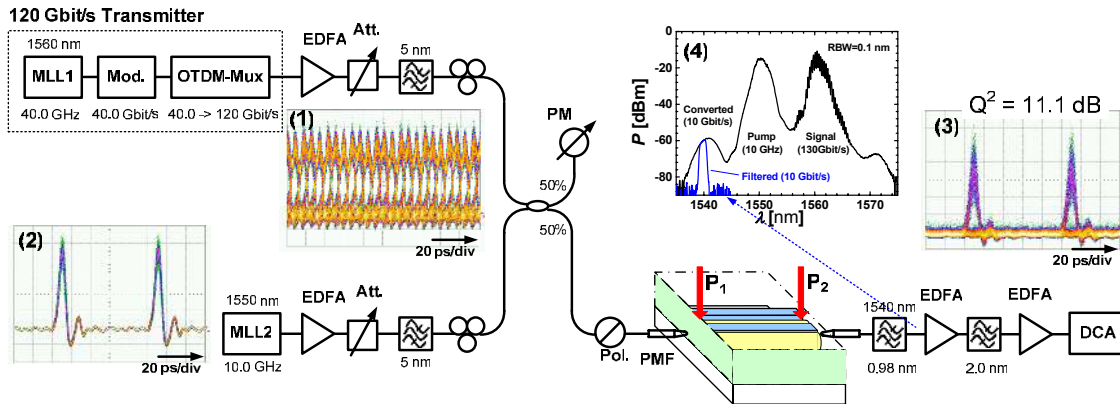


Fig. 2 Experimental setup of the demultiplexing experiment. MLL1, MLL2 = mode-locked lasers, Mod = data modulator, OTDM-Mux = optical time-division multiplexer, EDFA = erbium-doped fiber amplifier, Att = attenuator, PM = power meter, Pol = polarizer, PMF = polarization maintaining fiber, DUT = device under test, DCA = digital communication analyzer. Insets: (1) 120 Gbit/s signal, (2) 10 GHz pump, (3) demultiplexed 10 Gbit/s signal, (4) Spectrum at the output of the DUT and after bandpass-filtering.

6. Summary

We have fabricated and characterized silicon nanophotonic slot waveguides using DUV lithography and standard CMOS processing. By functionalization with an organic cladding material, we obtain a record nonlinearity of $104\,000\text{ W}^{-1}\text{km}^{-1}$ in the $1.5\ \mu\text{m}$ telecommunication window. We demonstrated the viability of such devices for all-optical signal processing by demultiplexing a 120 Gbit/s data stream to 10 Gbit/s using degenerate FWM with 15.6 dBm on-chip pump power. While this is to the best of our knowledge the first time that functionalized SOI slot waveguides were tested in high-speed optical communication systems, we believe that there is a large potential of improving the signal quality and the conversion efficiency.

7. Acknowledgement

This work was supported by the Center for Functional Nanostructures (CFN) of the Deutsche Forschungsgemeinschaft (DFG), by the Initiative of Excellence of the University of Karlsruhe, and by the European project TRIUMPH (grant IST-027638 STP). We acknowledge technological support by ASML Netherlands B.V. and equipment loan from Siemens Portugal and from Optoelectronics Research Centre (ORC) in Southampton, UK.

8. References

- [1] Julie Y.Y. Leong, Periklis Petropoulos, Symeon Asimakis, Heike Ebendorff-Heidepriem, Roger C. Moore, Ken Frampton, Vittoria Finazzi, Xian Feng, Jonathan H.V. Price, Tanya M. Monro, David J. Richardson, "A lead silicate holey fiber with $\gamma = 1860\text{ W}^{-1}\text{km}^{-1}$ at 1550 nm"; Proc. OFC'2005, March 2005
- [2] E. C. Mägi, L.B. Fu, H.C. Nguyen, M.R.E. Lamont, D. I. Yeom, B.J. Eggleton; "Enhanced Kerr nonlinearity in sub-wavelength diameter As₂Se₃ chalcogenide fiber tapers"; Optics Express **15**, 10324-10329 (2007).
- [3] V. G. Ta'eed, M. D. Pelusi, B. J. Eggleton, D.-Y. Choi, S. Madden, D. Bulla and B. Luther-Davies, "Broadband wavelength conversion at 40 Gb/s using long serpentine As₂S₃ planar waveguides," Opt. Express **15**, 15047-15052 (2007).
- [4] R. Salem, M. A. Foster, A. C. Turner, D. F. Geraghty, M. Lipson and A. L. Gaeta, "Signal regeneration using low-power four-wave mixing on silicon chip", Nature Photonics, **2**, 35-38 (2008)
- [5] M. Hochberg, T. Baehr-Jones, G. Wang, M. Shearn, K. Harvard, J. Luo, B. Chen, Z. Shi, R. Lawson, P. Sullivan, A. K. Y. Jen, L. Dalton and A. Scherer, "Terahertz all-optical modulation in a silicon-polymer hybrid system," Nature Materials **5**, 703-709 (2006).
- [6] C. Koos; L. Jacome; C. Poulton; J. Leuthold, and W. Freude, "Nonlinear silicon-on-insulator waveguides for all-optical signal processing", Opt. Express **15**, 5976-5990 (2007).
- [7] W. Bogaerts, P. Dumon, D. Van Thourhout, D. Taillaert, P. Jaenen, J. Wouters, S. Beckx, and R. Baets, "Compact wavelength-selective functions in silicon-on-insulator photonic wires", J. Selected Topics in Quantum Electronics, **12**, 1394-1401 (2006).
- [8] Y.-H. Kuo, H. Rong, V. Sih, S. Xu, M. Paniccia, and Oded Cohen, "Demonstration of wavelength conversion at 40 Gb/s data rate in silicon waveguides," Opt. Express **14**, 11721-11726 (2006).
- [9] T. Michinobu, J. C. May, J. H. Lim, C. Boudon, J.-P. Gisselbrecht, P. Seiler, M. Gross, I. Biaggio and F. Diederich, "A new class of organic donor-acceptor molecules with large third-order optical nonlinearities", Chem. Commun., 737-739 (2005)